Batteries & Supercaps

Research Article
doi.org/10.1002/batt.202500394

Chemistry Europe
European Chemical Societies Publishing

www.batteries-supercaps.org

Molecular Mechanism of Ionic Conductivity Enhancement by Heterogeneous Interface in Composite Hydrogel Electrolytes

Hongdeok Kim, Sihyun Kim, Junho Oh, and Joonmyung Choi*

Enhancing ion transport in polymer hydrogels is essential for the development of hydrogel-based electrochemical devices. Herein, this study investigates the molecular mechanisms by which embedded SiO_2 nanoparticles enhance the ionic conductivity of poly(acrylic acid) (PAA) hydrogels. Upon hydration, the deprotonated PAA chains expand the intermolecular space through electrostatic repulsion. Concurrently, the strong surface energy of SiO_2 drives the formation of solvent-enriched interfacial water channels. These interfacial structures facilitate ion transport via two synergistic effects: 1) Zn^{2+} ions near the nanoparticle interface experience reduced structural constraints from the polymer network, and 2) the hydration shells of interfacial Zn^{2+} ions are partially disturbed and asymmetric, weakening the ion-water binding. These nanoscale alterations reduce both steric hindrance and solvation energy barriers, resulting in enhanced Zn^{2+} mobility within the hydrogel domains. This work provides a mechanistic framework for understanding nanoparticle–hydrogel interactions and offers insights into the design of composite hydrogel electrolytes with enhanced ion-transport performance.

1. Introduction

Advancements in polymer-based electrolytes are central to the development of next-generation electrochemical energy storage systems.[1–3] Among the various candidates, hydrogel electrolytes, which comprise 3D water-swollen polymer networks, have emerged as a promising class of materials that combine high ionic conductivity with enhanced mechanical stability.[4–6] Unlike traditional liquid electrolytes, hydrogels inherently prevent leakage, suppress solvent volatilization, and maintain their structural integrity under mechanical deformation.[7] Their intrinsic flexibility and processability render them attractive for applications in flexible electronics and wearable devices.[8] However, conventional hydrogels often suffer from limited ionic conductivity owing to the dense entanglement of polymer chains and strong interactions between hydrated ions and the polymer matrix.[9] Therefore, overcoming transport limitations while preserving mechanical robustness remains a key challenge in the design of high-performance hydrogel electrolytes.

To address these challenges, recent studies have focused on incorporating inorganic nanoparticles into polymer hydrogels to form nanocomposite hydrogel electrolytes.[10–12] Nanoparticles with high surface energy, such as MXene, SiO_2, and graphene oxide, can locally reorganize the hydrogel microstructure to enhance transport efficiency.[13–15] The strong interactions between the nanoparticles and hydrogel chains can dissociate the condensed crystalline phase.[16] This suggests that the absorption capacity of liquid electrolytes can be enhanced by increasing the free volume fraction in the hydrogel matrix. Moreover, the nanoparticles can stabilize the absorbed solution by trapping adjacent water molecules. This facilitates the formation of solvent-rich domains near the surfaces, which function as preferential ion conduction paths decoupled from the polymer network. Beyond improving ionic conductivity, nanoparticle incorporation has also been shown to enhance mechanical integrity by increasing fatigue resistance and fracture toughness and suppressing swelling deformation.[17–20]

Ion transport in hydrogel electrolytes is fundamentally governed by the interplay between ionic coordination and polymer network dynamics.[21–23] In a hydrated environment, ions reside in transient coordination environments and form local solvation shells by associating with water molecules and polar functional groups on the polymer chains. Ion migration primarily occurs via a hopping mechanism, in which an ion continuously exchanges

H. Kim, J. Choi
School of Mechanical Engineering
Sungkyunkwan University
Suwon 16419, Republic of Korea
E-mail: joonchoi@skku.edu

S. Kim, J. Oh
Department of Mechanical Design Engineering
Hanyang University
222 Wangsimni-ro, Seongdong-gu, Seoul 04763, South Korea

S. Kim, J. Oh
Department of Mechanical Engineering
BK21 FOUR ERICA-ACE Center
Hanyang University
55 Hanyangdaehak-ro, Sangnok-gu, Ansan, Gyeonggi-do 15588, South Korea

Supporting information for this article is available on the WWW under https://doi.org/10.1002/batt.202500394

Research Article
doi.org/10.1002/batt.202500394
Chemistry Europe
European Chemical Societies Publishing

its coordination partners.[24–26] This process is closely coupled to the segmental motion of the polymer matrix and is sensitive to local microstructural features. The introduction of nanoparticles generates interfacial regions where both the polymer structure and ionic environment deviate from those of the bulk hydrogel, potentially altering the coordination configurations and transport dynamics.[27,28] However, despite the promising impacts of these interfacial modifications, the molecular mechanisms by which nanoparticles influence ionic conduction in hydrogel electrolytes remain poorly understood.

In this study, we systematically investigated the molecular mechanisms by which SiO_2 nanoparticle incorporation modulates ion transport in poly(acrylic acid) (PAA) hydrogel electrolytes. Through combined morphological and ion coordination analyses, we elucidated how nanoparticle-induced structural reorganization altered the local polymer environment and hydration dynamics of mobile ions. We demonstrated that the formation of interfacial water-rich channels alleviated the steric confinement imposed by the hydrogel network, and the disruption of the hydration shell structures weakened the ion-water binding. These findings provide critical molecular-level insights into the design principles of nanocomposite hydrogel electrolytes and contribute to the development of next-generation flexible energy storage systems.

2. Experimental Section

A molecular model of a pure PAA hydrogel was constructed in an all-atomic molecular dynamics (MD) simulation environment. The PAA chain consisted of 208 acrylic acid repeating units, which corresponded to a molecular weight of 14991.1 g mol^{-1} (**Figure 1**a). To avoid unnecessary intermolecular overlaps during the initial arrangement process, 20 PAA chains were arranged in the simulation box at a low density of 0.1 g cm^{-3}. Periodic boundary conditions were applied in all directions. Then, the box size was uniformly reduced to increase the system density to 1.0 g cm^{-3}. For every 0.1 g cm^{-3} increase in density, an energy optimization with an energy cutoff of 10 kcal mol^{-1} was applied. For the condensed PAA model, the NVT ensemble was performed for 0.5 ns at 300 K, followed by the NPT ensemble for 2 ns at 300 K and 1 atm. To relieve the internal residual stress, the model was heat-treated at 700 K for 2 ns under NPT conditions and then equilibrated back to room temperature. Atomistic modeling of the PAA-SiO_2 hydrogel was performed using the same procedure, with a spherical SiO_2 nanoparticle with a radius of 14 Å inserted at the center of the unit cell. The surface of the SiO_2 nanoparticle was treated with —OH termini.

A gradual hydration was performed on the equilibrated hydrogel models. A set of water molecules corresponding to 25 wt% of the PAA chains was prepared and randomly distributed in each hydrogel model. Simultaneously, 20% of the PAA carboxyl groups were deprotonated, and Zn^{2+} ions with the same charge weight were inserted to maintain the charge balance. The hydrogel models were then subjected to relaxation at 300 K and 1 atm for 10 ns. This process was repeated until the total weight fraction of water molecules reached 125 wt%, which is equal to the experimental swelling ratio (Figure 1b).[29] The corresponding changes in the simulation cell dimensions are shown in Figure S1, Supporting Information.

In this simulation model, crosslinking agents in hydrogel matrix are intentionally omitted even though they are essential in typical experimental approaches. The most important purpose of using crosslinking agents is the prevention of dissolution upon hydration. Since hydrophilic polymers, including PAA, tend to completely fill their surroundings with water molecules, entanglement and complete dissociation between polymer chains are frequently observed during the water absorption process. However,

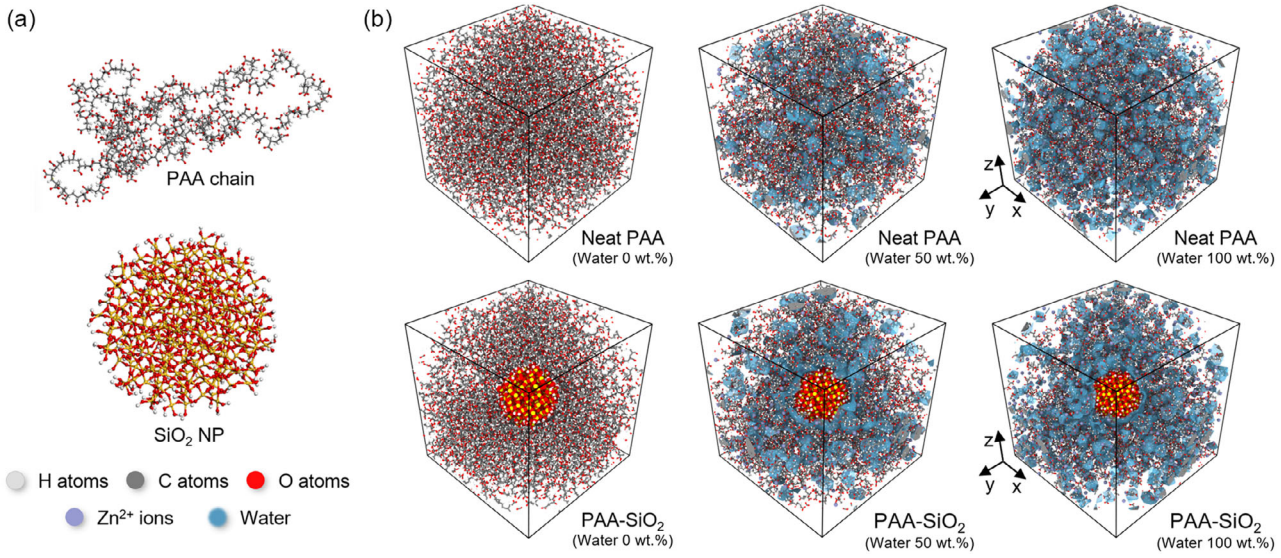

Figure 1. Microstructural fabrication of polymer nanocomposite hydrogels. a) Atomistic structure of single PAA chain and spherical SiO_2 nanoparticle. b) Molecular configuration of equilibrated neat PAA and PAA-SiO_2 hydrogels at varying hydration levels. Water molecules are highlighted as sea-blue surfaces.

in our MD simulations, we allowed exactly the same number of water molecules in both neat PAA and nanocomposites models to focus only on the surface effects due to nanoparticles. In other words, indiscriminate penetration of water and solvent molecules which potentially cause dissolution of hydrogel was completely controlled; the purpose of using a crosslinking agent is unclear in the current simulation model. Furthermore, due to the low concentration of crosslinking agent (typically below 3% in mass fraction[30]), only a small number of molecules can be present in the currently fabricated nanoscale models. Their spatial distribution determined by the initial random positioning during the modeling procedure can unintentionally govern the characteristics of interfacial or bulk properties. For these reasons, the crosslinking agent is ignored for the simplification of the system.

The dimensional changes of PAA and PAA- SiO_2 during water absorption were investigated (**Figure 2**). Both hydrogel models exhibited linear expansion strains depending on water content. Notably, the nanocomposite hydrogel exhibited a lower swelling strain than neat PAA, in good agreement with other studies reporting that nanoparticle insertion contributed to the dimensional stability of the hydrogel.[31]

We performed a thorough comparative analysis between our simulation conditions and the relevant experimental data reported in the literature (Table S1, Supporting Information). First, it can be confirmed that the material composition conditions adopted in this study (i.e., molecular weight of PAA and SiO_2 filler content) faithfully follow the conditions considered experimentally. Second, the fundamental material properties (i.e., mass density and swelling ratio) in dry and hydrated states also show high quantitative agreement with the experimental values. Still, one limitation is that the macroscopic behaviors of the considered system as a hydrogel electrolyte are sensitive to the process environment and experimental methods. Therefore, we assessed qualitative trends in material behavior as a complementary approach (Table S2, Supporting Information). The correlation between the volume expansion of the material and the change in ionic conductivity during the hydration process both qualitatively but clearly followed the experimental observations. The only discrepancy is the water absorbency, which can be justified as our study precisely controlled the number of water molecules to focus on the effect of the nanoparticle interface.

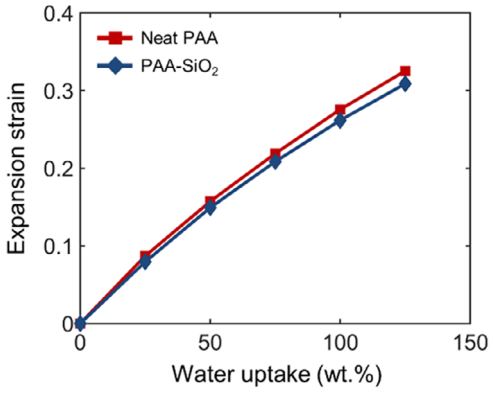

Figure 2. Water-induced expansion strain of neat PAA and PAA-SiO_2 nanocomposite hydrogels.

Atomistic modeling of PAA and PAA-SiO_2 was performed in Materials Studio 2020 (Dassault Systèmes, France). Subsequent hydration simulations were performed using open-source LAMMPS MD software (Sandia National Laboratories, USA).[32] The interatomic interactions of PAA and SiO_2 were described using the Polymer Consistent Force Field (PCFF).[33] Water molecules were described by the TIP3P potential.[34] Noncovalent interactions between water and the nanocomposite components were described by the 9-6 Lennard-Jones potential embedded in the PCFF.

3. Results and Discussion

3.1. Morphological Characterization of Neat PAA Hydrogel

The structural evolution of the neat PAA hydrogel upon water absorption was systematically analyzed. In the dehydrated state, PAA exhibited a densely packed microstructure, driven by extensive hydrogen bonding among carboxylic acid groups (density: 1.41 g cm^{-3} in molecular simulations and 1.40 g cm^{-3} experimentally[35]). Upon hydration, deprotonation of the carboxyl groups induced electrostatic repulsion along the polymer backbone, effectively disrupting the hydrogen-bonding network and increasing the interchain spacing. This structural rearrangement decreased the polymer density within the unit cell (**Figure 3**a). The enlarged free volume generated by the interchain expansion enabled the infiltration of external species. Consequently, the interstitial spaces were uniformly filled with water molecules and Zn^{2+} ions, forming a hydrated ion-conductive matrix (Figure 3b).

To elucidate the molecular-scale interactions between the PAA chains and infiltrating species, radial distribution function (RDF) analyses were conducted (Figure 3c). The RDF profile shows that Zn^{2+} ions were preferentially located around the PAA chains. In addition, the RDF formed by PAA-Zn^{2+} has sharp and narrow peaks, suggesting localized adsorption based on strong coordination bonds. The valleys between adjacent peaks in the RDF profiles are broad, indicating that the amorphous PAA chains encapsulated and spatially isolated the Zn^{2+} ions. The findings indicate that the deprotonated carboxylate groups acted as highly active adsorption sites for Zn^{2+}, contributing to its immobilization within the hydrogel network.

The RDF profile of PAA and water molecules has a completely different shape from that of PAA and Zn^{2+}, exhibiting broader and less sharp peaks that indicate weaker and more dynamic interactions. In other words, the spatial arrangement of water molecules was primarily determined by strong electrostatic interactions with Zn^{2+} ions and secondarily by PAA chains. A key structural motif of water molecules during interaction with metal ions is the formation of octahedral hydration shells.[36] Such an octahedral configuration appeared in the interfacial region between PAA and Zn^{2+} (see inset of Figure 3b). This partial retention of the hydration layer served

Research Article
doi.org/10.1002/batt.202500394
Chemistry Europe
European Chemical Societies Publishing

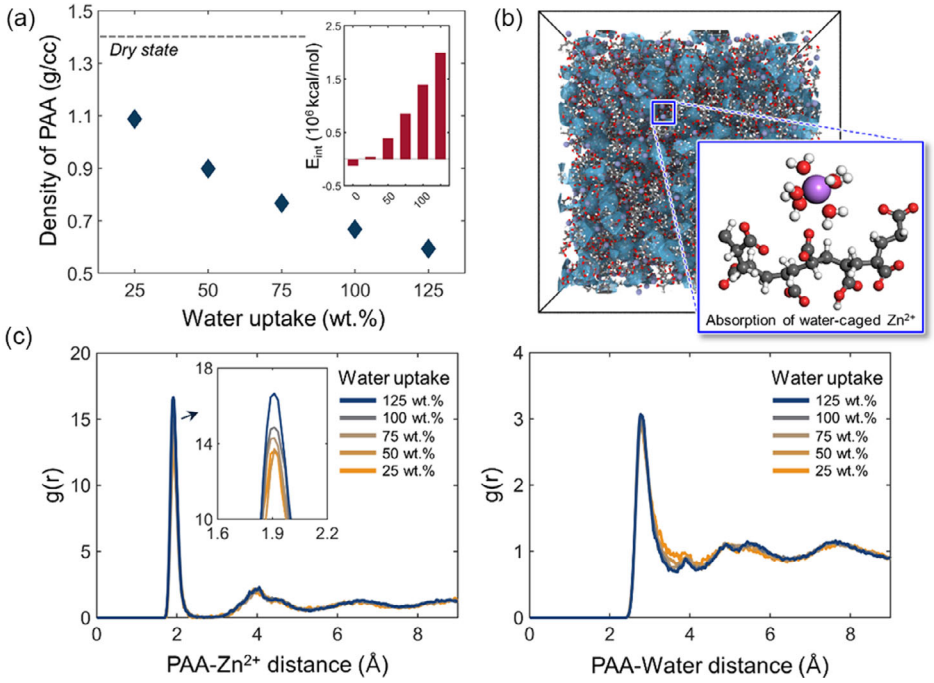

Figure 3. Morphological characterization of neat PAA upon water absorption. a) Change in effective density of PAA molecules. The intermolecular interaction energies between PAA molecules are shown in the inset. b) Molecular snapshot of neat PAA microstructure at a water content of 100 wt%. c) Radial distribution function (RDF, $g(r)$) of PAA-Zn^{2+} (left) and PAA-water (right) at different water contents.

to shield direct PAA–Zn^{2+} interactions, thereby facilitating effective ion transport within the polymer matrix.

3.2. Nanoparticle-Induced Morphological Change in PAA-SiO_2 Hydrogel

To investigate the morphological evolution of the hydrogel matrices due to the insertion of nanoparticles, the radial density distribution of the individual hydrogel components was analyzed (**Figure 4**a). In the anhydrous state (0 wt% water), the PAA chains exhibited a strong affinity for the SiO_2 surface, forming a compact adsorbed layer with a peak density of 1.8 g cm^{-3} at ≈2 Å from the interface. This dense interfacial layer arose from the thermodynamic compatibility based on hydrogen bonding between the carboxyl group and the —OH termini of the nanoparticles. Subsequently, the PAA density plateaued at ≈1.4 g cm^{-3} at ≈6 Å, where the van der Waals interactions with the nanoparticles disappeared.[37,38]

After hydration (50 wt% water), partial deprotonation of the carboxylic acid groups led to the generation of negatively

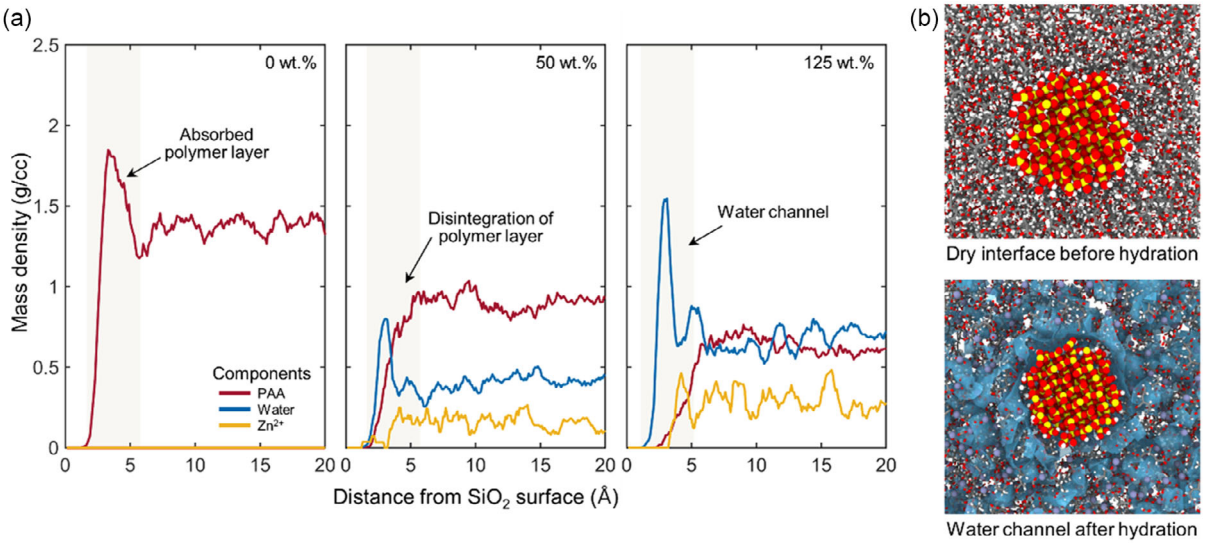

Figure 4. Nanoparticle-induced morphological change in PAA-SiO_2 hydrogels. a) Radial density distribution of PAA-SiO_2 hydrogel components. b) Molecular snapshots of the SiO_2-PAA interface in dry and wet conditions (water content: 125 wt%).

Research Article
doi.org/10.1002/batt.202500394
Chemistry Europe
European Chemical Societies Publishing

charged carboxylates, which induced strong electrostatic repulsion between adjacent polymer chains. These electrostatic repulsions disrupted the condensed microstructure; the effect was particularly significant in the interfacial region, where the molecules were close to each other. Therefore, the PAA showed a pronounced decrease in density near the SiO_2 surface.

At higher hydration levels (125 wt% water), the interfacial polymer layer was fully destabilized. The hydrophilic —OH terminals of SiO_2 filled the enlarged free space at the interface with water molecules and Zn^{2+} ions, resulting in the formation of a solvent-rich interphase. This structural transition was further supported by the molecular configuration. The PAA-SiO_2 interface, which is equilibrated in the dry state, transformed into a hydrated region densely populated with water and Zn^{2+} ions after sufficient water intrusion (Figure 4b). Notably, the Zn^{2+} ions remained solvated within hydration shells, maintaining their coordination shells even in the crowded interfacial region. Therefore, the immediate vicinity of the nanoparticles was occupied by abundant water molecules, followed by the peak concentration of Zn^{2+} ions. Beyond ≈6 Å, the component distributions converged to values that indicated the equilibrium state of the bulk hydrogel matrix.

Previous studies have suggested that these locally densified water layers can act as a low-resistance diffusion path to facilitate efficient ion transport, that is, behave as a "channel".[39] However, the underlying mechanism of the enhanced ion diffusion remains unclear. Therefore, in the following section, we analyze the nanostructural mechanism by which interfacial water channels by heterogeneous fillers enhance ion transport.

3.3. Molecular Mechanism of Ion Transport Enhancement at the PAA/SiO_2 Interface

The above structural analysis clearly shows that the nanoparticle-induced interaction force significantly modulates the nanoscale morphology of the interface. In this section, the molecular mechanisms by which the interfacial water channels contribute to the enhancement of ion conductivity are explored. Practical ion transport occurs when the ions encapsulated in the hydration shell overcome the anchoring forces of the hydrogel chains. Therefore, the analysis focuses on two structural parameters of Zn^{2+}: the structural constraints imposed by the PAA chains and the shell structure of the surrounding water molecules.

The interaction energy of Zn^{2+} ions with respect to their location within the hydrogel matrix was evaluated (**Figure 5**a), and the results were decomposed into the individual contributions of the hydrogel components. In both the bulk and interface, most of the energy came from interactions with the PAA chains. Importantly, interfacial Zn^{2+} ions had substantially weaker interactions with the hydrogel components, particularly with the PAA chains. The Zn^{2+} ions located in the bulk matrix were surrounded by a densely entangled PAA network, which imposed high structural constraints and limited ion mobility (Figure 5b). In contrast, at the polymer–nanoparticle interface, the formation of interfacial water channels disrupted the continuity of the hydrogel network, thereby alleviating steric confinement.

To further probe the mechanical environment experienced by Zn^{2+} ions under an external field, we monitored the evolution of stress on the ions during the application of an electric field (Figure 5c). An external field in the range of 0–4 V $Å^{-1}$ was applied along the *z*-direction of the unit cell under the NVT ensemble at 300 K. The atomic stress tensor of the Zn^{2+} ions was determined based on the virial theory.[40] In the bulk region, the stress on Zn^{2+} ions remained relatively unchanged, but in the interfacial region, the stress showed a gradual and monotonic decrease with increasing field strength. This continuous decrease implies that interfacial Zn^{2+} ions experienced less mechanical resistance to displacement under the electric field owing to the more flexible and less entangled polymer environment.

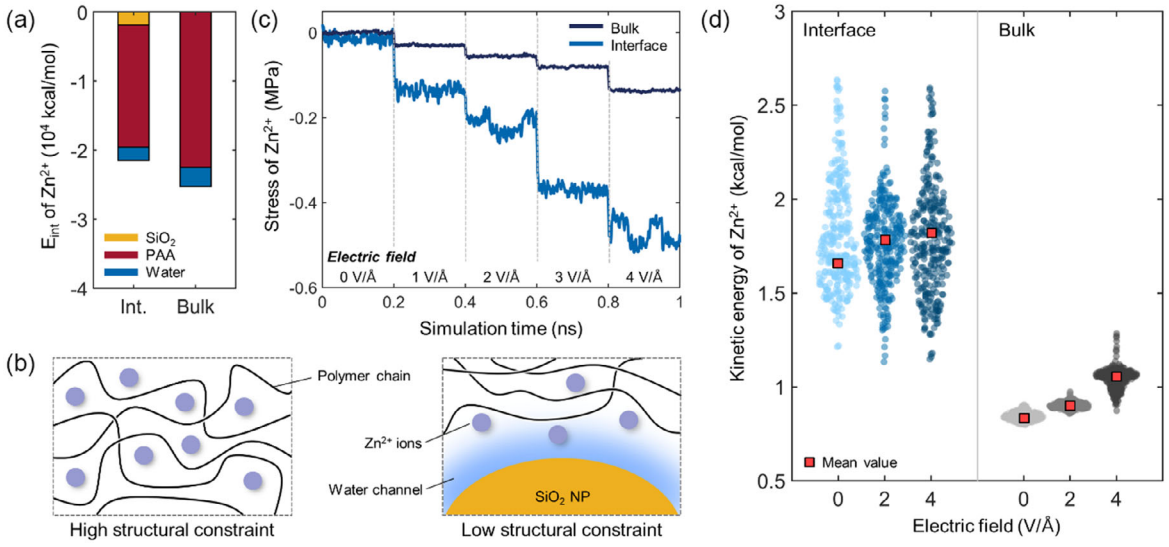

Figure 5. Changes in structural constraints of Zn^{2+} ions due to the formation of interfacial water channels. a) Measurement of the interaction energy (E_{int}) between the hydrogel components and Zn^{2+} ions. b) Schematics of Zn^{2+} ions located in the bulk matrix (left) and at the interface (right). c) Stress evolution of bulk and interfacial Zn^{2+} under the application of an electric field. d) Variation in kinetic energy of Zn^{2+} ions.

In agreement with the above, the kinetic energy of Zn^{2+} ions at the interface was significantly higher than that in the bulk across all field strengths (Figure 5d). The elevated kinetic energy indicates reduced steric hindrance and lower molecular friction, contributing to the enhancement of ionic mobility in the interfacial region. Notably, the energy distribution of the interfacial ions broadened with increasing field strength, indicating a more active and less constrained ion population. In contrast, the kinetic energy of bulk Zn^{2+} ions remained relatively low and invariant, consistent with their confinement within the dense hydrogel matrix.

To further investigate how the hydration structure affected the mobility of Zn^{2+} ions at the PAA–SiO_2 interface, the configuration of the hydration shell was quantitatively analyzed. For comparative purposes, the H_2O–Zn^{2+} model consisting only of water and Zn^{2+} was constructed. The number of water molecules constituting the hydration shell was determined based on a boundary of 2.4 Å, which corresponds to the Zn^{2+}–water equilibrium distance (**Figure 6**a). The H_2O–Zn^{2+} model represents an octahedral shell structure consisting of six water molecules.[41,42] By contrast, significantly fewer water molecules formed the primary hydration shell in the hydrogel environment. The reduction in hydration number indicated a partial disruption of the typical octahedral coordination structure of Zn^{2+} ions in hydrogel media, owing to the electrostatic interaction of Zn^{2+}–PAA. This disruption of the hydration shell was more prominent in the interfacial area; the competition of water–Zn^{2+} and water–SiO_2 interactions further reduced the structural stability of the hydration shell (Figure S2, Supporting Information, illustrates the disrupted hydration shells and the spatial distribution of Zn^{2+} ions in the vicinity of the nanoparticle). These observations were also supported by the decreased water–Zn^{2+} interaction energy at the interface, despite the identical coordination number (Figure S3, Supporting Information).

The effect of the disrupted shell structure has also been confirmed in previous studies.[43,44] The unsaturation of the coordination interaction leads to an asymmetric bonding structure between the metal ion and the solvent molecule. Such a distorted shell structure contributes to the increase in electrochemical conductivity and the decrease in overpotential. Similarly, the current results also confirm the mechanism that structural disruption and asymmetry of the hydration shell at the nanoparticle interface enhance the conductivity of Zn^{2+} ions.

This structural instability was also confirmed by the offset distance analysis (Figure 6b). The offset distance between the mass center of the hydration shell and the Zn^{2+} ion reflects the symmetry and stability of the hydration structure. In pure water, Zn^{2+} ions exhibit minimal offset, suggesting a highly symmetric and stable hydration shell. However, the offset distance increased markedly for Zn^{2+} in the PAA matrix and composite hydrogel. The interfacial Zn^{2+} ions showed higher offset distances than those in the bulk, suggesting unstable and asymmetric shell structures due to the spatial confinement of the nanoparticles.

The orientational dynamics of the water molecules within the hydration shell were examined via the H_2O–Zn^{2+} orientation angle as a function of the distance from the SiO_2 surface (Figure 6c). The orientation angle increased significantly near the surface (<5°), which is consistent with the above findings. Partial distortion of the hydration shell induced by the nanoparticles aggravated the structural instability of the water shell.

In conclusion, the interfacial Zn^{2+} ions were confirmed to reside in a structurally perturbed hydration environment. The disrupted hydration shells were beneficial for ionic conduction because they lowered the energy barrier required for ion migration. In bulk environments, the strongly bound hydration shells must be partially broken to allow ion transport, which is energetically inefficient. In contrast, the preweakened and flexible hydration shell at the interface facilitates more frequent reorganization events, thereby enabling faster translocation of Zn^{2+} ions. Furthermore, the small effective size of the predisturbed hydration ions was beneficial for their penetration into the tight spaces between the hydrogel chains. The present computational analysis

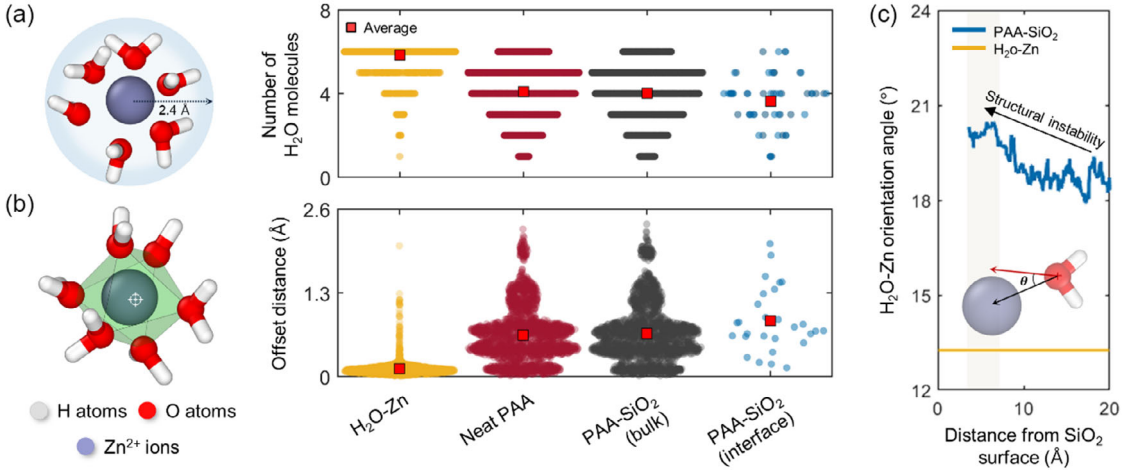

Figure 6. Structural evaluation of the Zn^{2+} ion hydration shell. a) The number of water molecules constituting the hydration shell. b) Offset distance between the mass center of the hydration shell and the Zn^{2+} ion. c) Changes in the orientation angle of water molecules as a function of the distance from the SiO_2 surface.

successfully provides a molecular-level explanation for the enhanced ionic mobility observed at the PAA–SiO_2 interface.

4. Conclusion

In this study, we elucidated the molecular mechanism by which nanoparticle-induced morphology modulation enhances ion transport performance in polymer hydrogels. Upon hydration, the deprotonation of the PAA chains induces electrostatic repulsion, leading to increased intermolecular spacing within the polymer network. The high surface energy of the nanoparticles drives the local enrichment of solvent molecules, resulting in the formation of interfacial water channels. These interfacial nanostructures contribute to the improved ionic conductivity through two primary mechanisms: 1) Zn^{2+} ions located in the water channels experience reduced structural constraints. Zn^{2+} ions confined within the bulk hydrogel matrix are surrounded by a densely entangled PAA network, which imposes significant electrostatic hindrance. In contrast, the water channels at the hydrogel–nanoparticle interface disrupt the local continuity of the polymer network, thereby relieving steric confinement. 2) The hydration shells surrounding Zn^{2+} were structurally disturbed. The spatial confinement near the nanoparticle surface leads to partial disruption and asymmetry in the hydration shells of the interfacial Zn^{2+} ions. These perturbed hydration environments decrease the effective hydrodynamic radii of the ions and weaken the ion-water binding strength. Consequently, the structural destabilization of the hydration shell facilitates faster ion translocation within the hydrogel matrix.

The present findings provide molecular insight into how nanoparticle–polymer interfacial interactions alter the local solvation structure and reduce the physical constraints on ion mobility. This facilitates a nanoscale understanding of the inherent role of nanoparticles in modulating the ionic conductivity of hydrogel-based electrolytes. The ionic conductivity of hydrogel electrolytes is further affected by particle geometry including size and agglomerated structure.[45] Therefore, our research is moving toward establishing mesoscale simulation frameworks for quantitative estimation of the performance of hydrogel electrolytes. Coarse-grained MD or dissipative particle dynamics will be introduced in the near future for probing particle–particle correlations and large-scale transport pathways and providing mesoscale microstructure design guidance.

Acknowledgements

This study was supported by the National Research Foundation of Korea (NRF) grant (no. RS-2023-00210865, no. RS-2023-00259994) funded by the Korean government (MSIT).

Conflict of Interest

The authors declare no conflict of interest.

Author Contributions

Hongdeok Kim: methodology, data curation, software, visualization, and writing of the original draft. **Sihyun Kim**: data curation, software, visualization, and writing of the original draft. **Junho Oh**: supervision, project administration. **Joonmyung Choi**: conceptualization, supervision, writing—review and editing. **Hongdeok Kim** and **Sihyun Kim** contributed equally to this work.

Data Availability Statement

The data that support the findings of this study are available from the corresponding author upon reasonable request.

Keywords: composite hydrogel electrolytes · interfacial interaction · ionic conductivity · molecular dynamics simulation

[1] Q. Liu, R. Liu, C. He, C. Xia, W. Guo, Z.-L. Xu, B. Y. Xia, *eScience* **2022**, *2*, 453.
[2] K. D. Fong, J. Self, B. D. McCloskey, K. A. Persson, *Macromolecules* **2021**, *54*, 2575.
[3] W. Zixuan, C. Jianxiong, F. Jialong, L. Zhiyong, G. Xin, *Energy Mater.* **2024**, *4*, 400050.
[4] Z. Wang, H. Li, Z. Tang, Z. Liu, Z. Ruan, L. Ma, Q. Yang, D. Wang, C. Zhi, *Adv. Funct. Mater.* **2018**, *28*, 1804560.
[5] W. Zhang, P. Feng, J. Chen, Z. Sun, B. Zhao, *Prog. Polym. Sci.* **2019**, *88*, 220.
[6] Y. Yamada, J. Wang, S. Ko, E. Watanabe, A. Yamada, *Nat. Energy* **2019**, *4*, 269.
[7] F. Mo, C. Mangwei, H. Ning, C. Lina, F. Jinbo, M. Zhiyuan, Y. Suzhu, W. Jun, Y. Huang, *Mater. Res. Lett.* **2022**, *10*, 501.
[8] M. Hina, S. Bashir, K. Kamran, F. Almomani, J. Ahmad, F. Kamarulazam, S. Ramesh, K. Ramesh, M. A. Mujtaba, *J. Energy Storage* **2024**, *85*, 110961.
[9] H. Wang, Z. Hou, Y. Wang, H. Long, D. Zhang, Z. Fu, N. Wu, Z. Zhai, B. Wang, *Chem. Eng. J.* **2025**, *510*, 161766.
[10] Y. Niu, X. Yuan, Y. Zhao, W. Zhang, L. Ren, *Macromol. Chem. Phys.* **2017**, *218*, 1600540.
[11] Y. Zhai, H. Duan, X. Meng, K. Cai, Y. Liu, L. Lucia, *Macromol. Mater. Eng.* **2015**, *300*, 1290.
[12] N. Moini, A. Jahandideh, G. Anderson, *Sustainable Polymer Composites and Nanocomposites* (Eds: S. Thomas Inamuddin, R. Kumar Mishra, A. M. Asiri), Springer International Publishing, Cham **2019**, pp. 805–853.
[13] Y.-Z. Zhang, J. K. El-Demellawi, Q. Jiang, G. Ge, H. Liang, K. Lee, X. Dong, H. N. Alshareef, *Chem. Soc. Rev.* **2020**, *49*, 7229.
[14] P. Tian, X. Zhong, C. Gu, Z. Wang, F. Shi, *Batteries* **2022**, *8*, 175.
[15] J. Wei, R. Wang, F. Pan, Z. Fu, *Sensors* **2022**, *22*, 3015.
[16] D. Lin, W. Liu, Y. Liu, H. R. Lee, P.-C. Hsu, K. Liu, Y. Cui, *Nano Lett.* **2016**, *16*, 459.
[17] S. Awasthi, J. K. Gaur, M. S. Bobji, C. Srivastava, *J. Mater. Sci.* **2022**, *57*, 8041.
[18] X. Nie, Y. Xie, X. Ding, L. Dai, F. Gao, W. Song, X. Li, P. Liu, Z. Tan, H. Shi, C. Lai, D. Zhang, Y. Lai, *Carbohydr. Polym.* **2024**, *334*, 122068.
[19] W.-C. Lin, A. Marcellan, D. Hourdet, C. Creton, *Soft Matter* **2011**, *7*, 6578.
[20] B. Xu, Y. Liu, L. Wang, X. Ge, M. Fu, P. Wang, Q. Wang, *Polymers* **2018**, *10*, 1025.
[21] Y. Hou, S. Ma, J. Hao, C. Lin, J. Zhao, X. Sui, *Polymers* **2022**, *14*, 4037.
[22] W. Chen, Q. Wang, J. Chen, Q. Zhang, X. Zhao, Y. Qian, C. Zhu, L. Yang, Y. Zhao, X.-Y. Kong, B. Lu, L. Jiang, L. Wen, *Nano Lett.* **2020**, *20*, 5705.
[23] L. Li, L. Zhang, W. Guo, C. Chang, J. Wang, Z. Cong, X. Pu, *J. Mater. Chem. A* **2021**, *9*, 24325.
[24] H. Najafi Fath Dehghan, A. Abdolmaleki, M. Pourahmadi, P. Khalili, A. R. Arvaneh, M. Sadat-Shojai, *J. Mol. Liq.* **2023**, *382*, 121860.
[25] H. Xia, G. Xu, X. Cao, C. Miao, H. Zhang, P. Chen, Y. Zhou, W. Zhang, Z. Sun, *Adv. Mater.* **2023**, *35*, 2301996.
[26] S. Hadad, M. A. Pope, M. Kamkar, K. C. Tam, *Adv. Sustain. Syst.* **2025**, *9*, 2400532.
[27] P. Fan, H. Liu, V. Marosz, N. T. Samuels, S. L. Suib, L. Sun, L. Liao, *Adv. Funct. Mater.* **2021**, *31*, 2101380.
[28] M. Dirican, C. Yan, P. Zhu, X. Zhang, *Mater. Sci. Eng. R-Rep.* **2019**, *136*, 27.

[29] Y. Ma, Y. Sun, Y. Fu, G. Fang, X. Yan, Z. Guo, *Chemosphere* **2016**, *163*, 610.
[30] R. A. McBath, D. A. Shipp, *Polym. Chem.* **2010**, *1*, 860.
[31] E. Ye, X. J. Loh, *Aust. J. Chem.* **2013**, *66*, 997.
[32] A. P. Thompson, H. M. Aktulga, R. Berger, D. S. Bolintineanu, W. M. Brown, P. S. Crozier, P. J. in 't Veld, A. Kohlmeyer, S. G. Moore, T. D. Nguyen, R. Shan, M. J. Stevens, J. Tranchida, C. Trott, S. J. Plimpton, *Comput. Phys. Commun.* **2022**, *271*, 108171.
[33] H. Sun, *J. Comput. Chem.* **1994**, *15*, 752.
[34] A. D. MacKerell Jr., D. Bashford, M. Bellott, R. L. Dunbrack Jr., J. D. Evanseck, M. J. Field, S. Fischer, J. Gao, H. Guo, S. Ha, D. Joseph-McCarthy, L. Kuchnir, K. Kuczera, F. T. K. Lau, C. Mattos, S. Michnick, T. Ngo, D. T. Nguyen, B. Prodhom, W. E. Reiher, B. Roux, M. Schlenkrich, J. C. Smith, R. Stote, J. Straub, M. Watanabe, J. Wiórkiewicz-Kuczera, D. Yin, M. Karplus, *J. Phys. Chem. B* **1998**, *102*, 3586.
[35] J. Li, G. van Ewijk, D. J. van Dijken, J. van der Gucht, W. M. de Vos, *ACS Appl. Mater. Interfaces* **2021**, *13*, 21844.
[36] V. Migliorati, G. Mancini, S. Tatoli, A. Zitolo, A. Filipponi, S. De Panfilis, A. Di Cicco, P. D'Angelo, *Inorg. Chem.* **2013**, *52*, 1141.
[37] H. Kim, J. Choi, *Compos. Pt. A-Appl. Sci. Manuf.* **2023**, *167*, 107461.
[38] S. Kim, H. Kim, J. Choi, *Compos. Pt. A-Appl. Sci. Manuf.* **2025**, *191*, 108720.
[39] K. W. Kim, H. Kim, J. Choi, S.-J. Choi, K. R. Yoon, *Energy Storage Mater.* **2024**, *71*, 103594.
[40] D. M. Heyes, *Phys. Rev. B* **1994**, *49*, 755.
[41] E. Cauët, S. Bogatko, J. H. Weare, J. L. Fulton, G. K. Schenter, E. J. Bylaska, *J. Chem. Phys.* **2010**, *132*, 194502.
[42] N. Díaz, D. Suárez, K. M. Merz Jr, *Chem. Phys. Lett.* **2000**, *326*, 288.
[43] C. Fu, L. Xu, F. W. Aquino, A. Cresce, M. Gobet, S. G. Greenbaum, K. Xu, B. M. Wong, J. Guo, *J. Phys. Chem. Lett.* **2018**, *9*, 1739.
[44] H. Kwon, Z. A. Ali, B. M. Wong, *Environ. Sci. Technol. Lett.* **2023**, *10*, 1017.
[45] Y. Ding, B. He, D. Wang, M. Avdeev, Y. Li, S. Shi, *Energy Mater. Adv.* **2023**, *4*, 0041.

Manuscript received: May 22, 2025
Revised manuscript received: July 10, 2025
Version of record online: